Infrastructural Materials

IMR KINKEN Research Highlights 2014

Investigation of 3D Atomic Local Structures around Dopants by Using Neutron Atomic-Resolution Holography

To investigate effects of doping in functional materials, we have developed the unique atomic-resolution neutron holography technique that can be used to observe local structures around light-element dopants. Because of the importance of light elements in functional materials, this technique will have a significant influence in the field of materials science.

In most functional materials, doping can control material performance; for instance, the characteristics of silicon as a semiconductor can be changed by a small amount of dopant such as boron or phosphorus. Thus, from the viewpoint of structural investigations, understanding the atomic structures around dopants is important.

The atomic-resolution holography (ARH) method is a unique probe for observing 3D local atomic structures around dopants [1,2]. The advantage of ARH over other methods is that the 3D local structures within ~20 Å around a selected atom can be visualized. Photoelectron and fluorescent X-rays ARH have been already in practical use in Japan. However, light elements such as boron or hydrogen, cannot be observed by electrons or X-rays accurately. Thus, we aim to develop the neutron ARH technique because neutrons have a much higher sensitivity to light elements.

Through collaboration with the IMR, we have succeeded in normal mode neutron ARH experiments of a $PdH_{0.78}$ single crystal and in visualizing the atomic structure around a hydrogen atom using a monochromatic neutron beam [1,2]. However, the accuracy of the atomic image was not sufficient because of the presence of imaging artifacts. To avoid imaging artifacts, we are developing a novel technique, the pulsed neutron ARH. We expect that multi-**λ** ARH can enhance accuracy of atomic images drastically since pulsed neutrons are white beams and a large number of holograms with different **λ** can be obtained at once.

In 2013, we performed the world's first pulsed neutron ARH experiments at Japan Proton Accelerator Research Complex (J-PARC), Tokai, Japan, and obtained clear holograms with different wavelengths. Figure 1 shows typical holograms from a single crystal of 1% Eu doped CaF_2, which is an important material for neutron scintillation counters. Some of the obtained holograms showed obvious linear structures, called standing wave lines, clearly (red arrows in Fig.1). The lines indicate the direction of (001) axes and show that we have succeeded in observing the symmetry of the local structure around Eu.

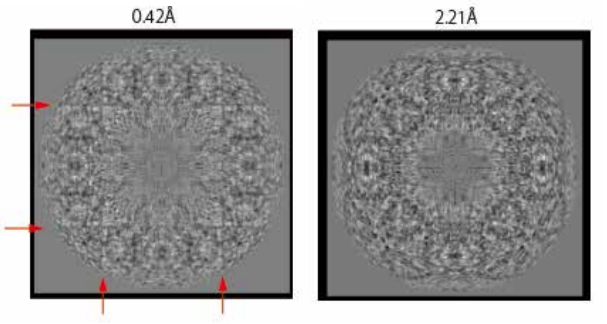

Fig.1 Holograms of $Ca_{0.99}Eu_{0.01}F_2$ with **λ**= 0.42 and 2.21 Å by pulsed neutron ARH in 2013. The red arrows indicate standing wave lines corresponding to the symmetry of the structure.

The results indicate that highly accurate local structure studies will be possible by neutron ARH at J-PARC. Because of the importance of light atoms in functional materials, neutron ARH will have a significant influence in the field of materials science. Tohoku University is now constructing a new neutron spectrometer [3] at J-PARC through collaboration with KEK, thus further improving the ARH technique.

References

[1] K. Hayashi, K. Ohoyama, S. Orimo, Y. Nakamori, H. Takahashi, and K. Shibata, Jpn. J. Appl. Phys. **47,** 2291 (2008).

[2] K. Hayashi and K. Ohoyama, Hyomen, **33,** 290 (2012). (Japanese)

[3] K. Ohoyama, T. Yokoo, S. Itoh, J. Suzuki, K. Iwasa, T.J. Sato, H. Kira, Y. Sakaguchi, T. Ino, T. Oku, K. Tomiyasu, M. Matsuura, H. Hiraka, M. Fujita, H. Kimura, T. Sato, J. Suzuki, H.M. Shimizu, T. Arima, M. Takeda, K. Kaneko, M. Hino, S. Muto, H. Nojiri, C.H. Lee, J.G. Park, and S. Choi, J. Phys. Soc. Jpn. **82,** SA036 (2013).

Keywords: doping, neutron scattering, structure
Kenji Ohoyama (Metal Physics with Quantum Beam Spectroscopy Division)
E-mail: ohoyama@imr.tohoku.ac.jp

Strengthening of Low-Carbon Steels by Nanoscopic Interphase Precipitates

Strengthening of steel components is required for weight reduction of automobiles. One of the most effective methods for increasing strength is precipitation strengthening with nanoscopic carbide particles. Our research group studied strengthening by interphase precipitation, in which nanoscopic alloy carbides are nucleated repeatedly at the interphase boundary during ferrite transformation. Here, we describe briefly the relationships between the crystallography of the transformation, the carbide dispersion, and the properties of a low-carbon steel with interphase precipitates.

When steels containing strong carbide-forming elements such as Nb, Ti, and V transform into ferrite, nanoscopic carbides nucleate repeatedly at interphase boundaries between ferrite and austenite during cooling; this is called interphase precipitation. Such precipitates have been used to strengthen medium-carbon forging steel [1] and low-carbon sheet steel [2, 3], which plays an important role in the weight reduction, and thus the improvement of the fuel efficiency, of automobiles.

Interphase precipitation takes place at ferrite/austenite boundary, and the characteristics of the boundary should strongly influence precipitation, although the details have yet to be clarified. Therefore, the relationships between the boundary coherency and the dispersion of the precipitates were investigated in addition to their effect on the strength. Coherency is measured as the angle of deviation from the coherent orientation relationship ($\Delta\theta$). The distribution of the interphase precipitates and the local hardness were co-characterized in individual ferrite grains to evaluate the effects of coherency by means of three-dimensional atom probe (3DAP) and nanoindentation methods, respectively.

Figure 1 shows 3DAP maps of V in a V-bearing low-carbon steel [2]. The blue clusters are vanadium carbides (VCs). In ferrite grains possessing good coherency with neighboring austenite grains, few VCs are observed, while a high density of VCs is present at incoherent boundaries. Figure 2(a) shows the variation in the number density of VC particles with $\Delta\theta$. VC nucleation is promoted by increasing $\Delta\theta$ up to 5°, and the density saturates at larger $\Delta\theta$. Thus, the coherency of the interface has a significant effect on interphase precipitation, presumably due to faster diffusion, higher interfacial energy, and more severe segregation at less coherent interfaces. Figure 2(b) shows the local hardness of the ferrite against $\Delta\theta$ [2]. The hardness increases with decreasing interfacial coherency, which agrees with the VC distribution results.

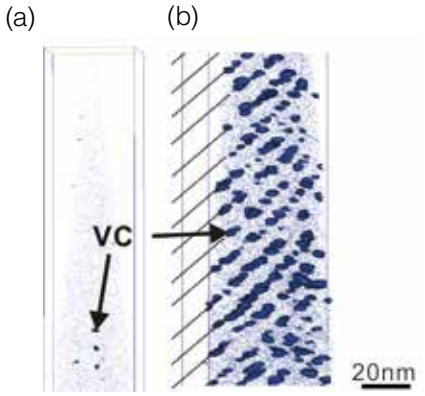

Fig. 1 3DAP maps of V atoms, showing the distribution of VC particles in the ferrite at (a) coherent and (b) less coherent boundaries with austenite [2].

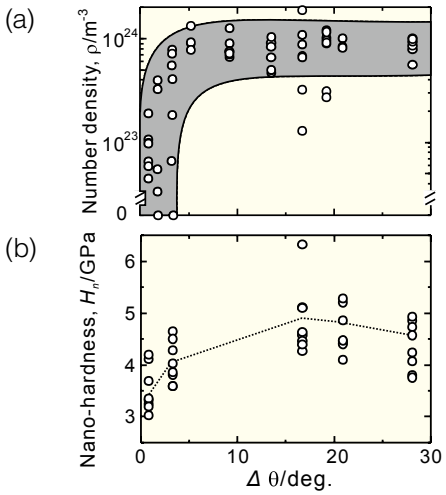

Fig. 2 Variation in (a) the number density of VCs and (b) the local hardness of the ferrite as a function of $\Delta\theta$ [2].

References

[1] G. Miyamoto, R. Hori, B. Poorganji, and T. Furuhara, Metall. Mater. Trans. A **44**, 3436 (2013).

[2] Y.-J. Zhang, G. Miyamoto, K. Shinbo, and T. Furuhara, Scripta Mater. **69**, 17 (2013).

[3] N. Kamikawa, Y. Abe, G. Miyamoto, T. Furuhara, and Y. Funakawa, ISIJ Int. **54**, 212 (2014).

Keywords: steel, strength, nanoparticle
Goro Miyamoto (Microstructure Design of Structural Metallic Materials Division)
E-mail: miyamoto@imr.tohoku.ac.jp
URL: http://www.st-mat.imr.tohoku.ac.jp/

Structure of Zr-Cu-Ag Metallic Glass Measured by Anomalous X-ray Scattering

The structures of Zr-Cu-Al metallic glasses were investigated using the anomalous x-ray scattering technique coupled with reverse Monte Carlo simulation (AXS-RMC). A Voronoi analysis showed that an improvement in the glass-forming ability of the Zr-Cu-Ag system appears to be associated with icosahedral coordination around Cu [1].

Recently, a multicomponent alloy system that forms bulk metallic glasses (BMGs) at a very low cooling rate has attracted much attention. In order to discuss the detailed chemical ordering units of an Al-Cu-Ag BMG, AXS-RMC analysis utilizing the anomalous dispersion effect near the absorption edge was carried out.

Alloy ingots in the Al-Cu-Ag system were prepared by arc melting. Ordinary X-ray diffraction and AXS measurements of the Cu, Zr, and Ag *K* absorption edges were carried out at BL-7C and NW10A of the Photon Factory at the Institute of Material Structure Science (IMSS), Tsukuba, Japan. As an example, the experimental interference functions $Qi(Q)$, $\Delta Qi_{Cu}(Q)$, $\Delta Qi_{Zr}(Q)$, and $\Delta Qi_{Ag}(Q)$, together with those obtained from AXS-RMC simulations for $Zr_{45}Cu_{45}Ag_{10}$, are shown in Fig.1.

The structural features obtained from the AXS-RMC simulation correspond well with those produced by the DRP model, implying that the fundamental structure of the Al-Cu-Ag glass could be well described based on the classical dense random packing structure. Additionally, the first peak position of each partial pair distribution function in the Zr-Cu-Ag glass corresponds to the sum of the Goldschmidt radii. These features are similar to those found in $Zr_{50}Cu_{50}$ amorphous alloy [2]. An icosahedral local ordering unit has been frequently suggested to describe the structural origin of the superior glass-forming ability (GFA) of these alloys, and the nearest-neighbor structures of the Al-Cu-Ag glass were carefully analyzed using the Voronoi tessellation method. The first nearest coordination number around Cu is the smallest, corresponding to that of an icosahedron. On the other hand, the coordination number around Zr is the largest, which corresponds to a body-centered cubic structure. However, no unique local atomic arrangement based on strong chemical ordering was developed upon addition of Ag.

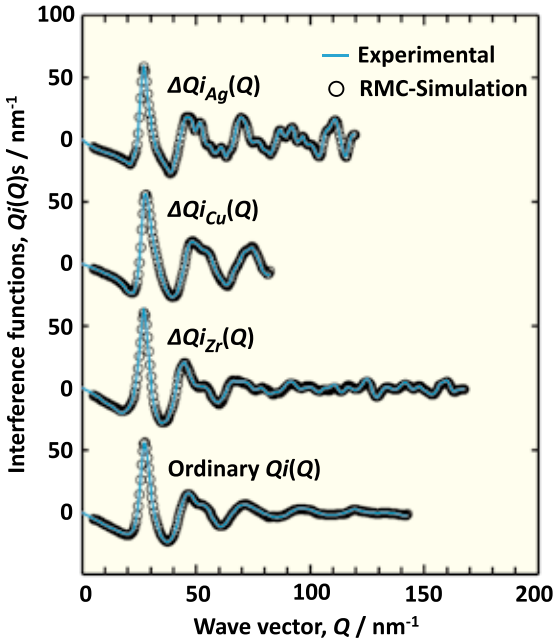

Fig. 1 Interference functions of $Zr_{45}Cu_{45}Ag_{10}$. The solid and dotted lines correspond to the experimental data and the data obtained using the AXS-RMC method, respectively.

The present Voronoi analysis indicates that the relative frequency of icosahedral coordination was largest around Cu in the $Zr_{45}Cu_{45}Ag_{10}$ BMG, for which superior glass-forming ability in the Zr-Cu-Ag system was reported. Therefore, an improvement in the glass forming ability of a Zr-Cu-Ag system appears to be associated with icosahedral local coordination.

References

[1] T. Kawamata, Y. Yokoyama, K. Sugiyama, and T. Fujita, Journal of Physics Conference Series **502**, 012027 (2014).

[2] T. Kawamata, Y. Yokoyama, M. Saito, K. Sugiyama, and Y. Waseda, Mater. Trans. **51**, 1796 (2010)

Keywords: bulk metallic glass, structure, anomalous X-ray scattering
Kazumasa Sugiyama (Chemical Physics of Non-Crystalline Materials Division)
E-mail: kazumasa@imr.tohoku.ac.jp
URL: http://www.xraylab.imr.tohoku.ac.jp/

High Fatigue Strength of Friction Stir-Welded Butt Joints Prepared Using a Newly Developed Titanium Alloy for Aircraft Applications

Friction stir welding (FSW) was applied in the butt joining of a newly-developed (α + β)-type Ti-4.5Al-2.5Cr-1.2Fe-0.1C alloy. The microstructure in the stir zone was controlled to obtain both equiaxed and acicular α structures by manipulating the welding parameters, such as the tool rotation speed and welding speed. Weld-defect–free joints were obtained by FSW, and a high fatigue strength, comparable to that of the parent plate, was obtained by combining FSW and annealing.

Friction stir welding (FSW) was applied in the butt joining of 2-mm-thick plates of the (α + β)-type titanium alloy Ti-4.5Al-2.5Cr-1.2Fe-0.1C (Ti531C) to improve the dynamic mechanical properties, such as fatigue strength, via the elimination of welding defects. The microstructure in the stir zone, either the equiaxed α or acicular α structure, was selected by manipulation of the welding parameters, namely the tool rotation speed and welding speed. A 700 °C anneal was performed after welding to release harmful residual stresses introduced during FSW. The microstructure and crystal texture both in the stir zone and in the base metal were analyzed using optical microscopy, scanning electron microscopy, field-emission electron probe X-ray microanalysis, and pole figure measurements obtained via X-ray diffraction methods. The stir zones of the Ti531C butt joints are harder than the base metals, both before and after annealing, because the crystal texture of the stir zones is different from that of the base metal. The tensile strengths and 0.2% proof stresses of the as-welded and annealed Ti531C butt joints are comparable to those of the Ti531C parent plate, while the elongation of both types of welded joints is lower than that of the Ti531C parent plate. The stir zones are harder than the base metal, which means that plastic deformation occurs mainly in the softer base metal region, as does the occurrence of failure, in each specimen. Conversely, failure occurs in the stir zone or at the boundary between the stir zone and base metal in the butt joints subjected to fatigue tests. This result implies that the tensile residual stresses introduced into the stir zone during FSW are the dominant factor in the fatigue failure of the Ti531C friction stir welded butt joints. Therefore, annealing to release the residual stresses is effective for improving the fatigue strength. In conclusion, the lack of pores or titanium carbide precipitates in the stir zones of the Ti531C friction stir welded butt joints with equiaxed α or acicular α structures, combined with the relaxation of internal stresses by annealing, results in almost no deterioration of the fatigue strength even after welding (Fig. 1).

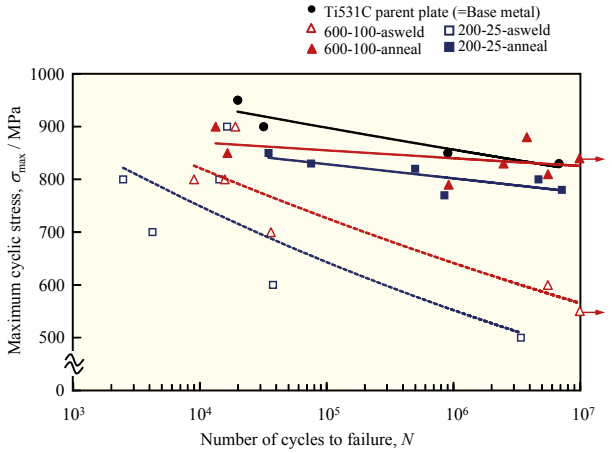

Fig. 1 Relationships between the maximum cyclic stress and number of cycles to failure of Ti531C friction stir welded butt joints. The “600-100” and “200-25” designations indicate tool rotation speed and welding speed, respectively.

References

[1] M. Nakai, M. Niinomi, J. Hieda, K. Cho, K. Komine, H. Fujii, Y. Morisada, Y. Ito, T. Konno, Y. Itsumi, H. Oyama, and W. Abe, Proceedings of the 1st International Joint Symposium on Joining and Welding, pp.429 (2013).

Keywords: metal, welding, fatigue
Mitsuo Niinomi (Biomaterials Science Division)
E-mail: niinomi@imr.tohoku.ac.jp
URL: http://biomat.imr.tohoku.ac.jp/

Ductile SiC/SiO_2 composite produced by a combination of chemical vapor deposition and spark plasma sintering

Silicon carbide is an attractive structural and functional material used in diverse applications. We fabricated ductile SiC/SiO_2 composites with a fine mosaic structure by a chemical vapor deposition-based powder-coating technique and spark plasma sintering. The SiC/SiO_2 composite was fully consolidated and exhibited high hardness and toughness.

Silicon carbide has excellent oxidation resistance, high thermal conductivity, and low activation under neutron irradiation; thus, SiC is a promising material for use in structural applications involving severe operating conditions, such as thermal protection tiles for space vehicles, diesel particulate filters, and fusion reactors. The drawbacks of SiC include its low fracture toughness and sinterability. To obtain bulk SiC materials, sintered SiC components usually contain additives such as boron, carbon, and aluminum to promote densification. However, these additives drastically degrade the oxidation resistance at high temperatures.

Developing a fine microstructure is crucial for enhancing the toughness of ceramic materials. Fine-microstructured ceramic composites, however, rarely form during conventional sintering procedures, i.e., simply mixing raw powders and heat treating them in a furnace. Our group has developed a technique called rotary chemical vapor deposition (rotary CVD) to deposit nanoscopic layers and particles on powder substrates. This technique enables us to develop finely structured and highly dispersed systems (Fig. 1(a)). We fabricated a SiC/SiO_2 composite powder with a SiC core/SiO_2 shell structure by rotary CVD, in which a nanoscopic layer of SiO_2 covered the surface of a SiC powder particle (Fig. 1(b)) [1, 2].

The core/shell-structured powder was consolidated at 1973 K by spark plasma sintering (SPS). The rapid densification and uniaxial pressure provided by SPS, in addition to the deposition of a continuous and well-adhered interface between the SiC and SiO_2, resulted in fully dense SiC-based composites. These SiC-based composites exhibited a high hardness of 17.1 GPa and fracture toughness of 8.4 MPa $m^{1/2}$ [2]. SiO_2 is soft and brittle; thus, it was thought that the SiC/SiO_2 composites would not exhibit such robust mechanical properties. However, by fully consolidating the mosaic microstructure, high-hardness, ductile SiC/SiO_2 composites were obtained. Because SiO_2 acts as a protective layer against high-temperature oxidation of SiC, these SiC/SiO_2 composites, lacking sintering additives, are promising for use as oxidation-resistant materials and give us new insight on oxidation behavior and mechanisms [3].

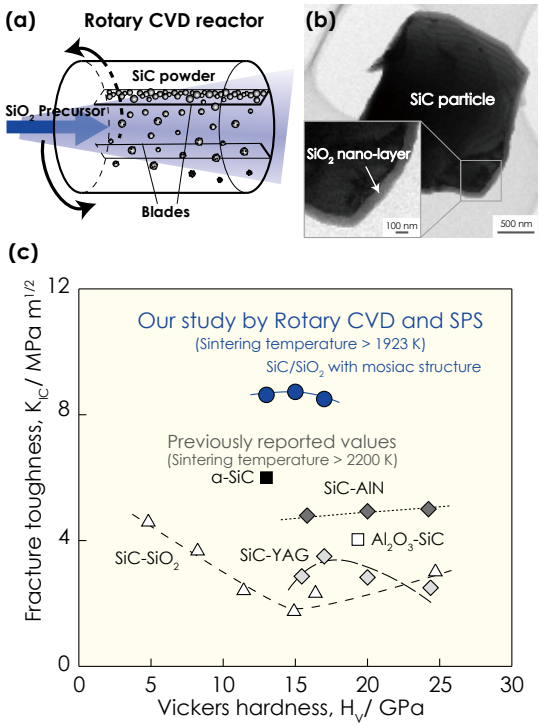

Fig.1 (a) Schematic diagram of the rotary CVD process, (b) SiC/SiO_2 core/shell composite powder fabricated by rotary CVD, and (c) the relationship between the fracture toughness and hardness of the densified SiC/SiO_2 composite in comparison with values in the literature.

References

[1] Z. He, H. Katsui, R. Tu, J. Zhang, and T. Goto, J. Am. Ceram. Soc. **97**, 681 (2014).

[2] Z. He, R. Tu, H. Katsui, and T. Goto, Int. Ceram. **39**, 2605 (2013).

[3] H. Katsui, M. Oguma, and T. Goto, Int. Ceram. J. Am. Ceram. Soc. **97**, 1633 (2014).

Keywords: chemical vapor deposition (cvd) (deposition), core/shell, sintering
Takashi Goto, Hirokazu Katsui, and Akihiko Ito (Multi-functional Materials Science Division)
E-mail: goto@imr.tohoku.ac.jp
URL: http://www.goto.imr.tohoku.ac.jp/

Additive Manufacturing Using Electron-Beam Melting and Novel Ni-Co-Cr-Mo Alloys Resistant to Severe Corrosive and Wear Environments

Cobalt-based alloys have been widely used in valve seats in nuclear power plants, aerospace fuel nozzles, and engine vanes, as well as orthopedic and dental implants because of their strength retention at high temperature, corrosion resistance, wear resistance, and biocompatibility. The additive manufacturing of components of a novel Ni-Co-Cr-Mo alloy by electron-beam melting was performed in the present study, and the corrosion resistance of the alloys, with and without added Co, to aqueous HF were compared and analyzed systematically for the first time.

Recently, electron-beam melting EBM has become an established process for additive manufacturing that can create complex three-dimensional (3D) structures from precursor metal powders. In the EBM process, a high-power electron beam is scanned across a powder substrate repeatedly to melt the metal powder selectively along a series of two-dimensional (2D) slices, forming a 3D object layer by layer.

The microstructures and high-temperature tensile properties of Co-28Cr-6Mo-0.23C-0.17N alloy components fabricated by EBM along cylindrical axes deviating from the build-direction by 0°, 45°, 55°, and 90° were investigated. The preferred crystal orientations of the γ phase in the as- built samples with deviation angles of 0°, 45°, 55°, and 90° were near [001], [110], [111], and [100], respectively (Fig. 1). $M_{23}C_6$ precipitates aligned along the build-direction at intervals of around 3 μm. The γ phase was completely transformed into a single ε-hcp phase after aging at 800 °C for 24 h, when lamellar colonies of M_2N precipitates and the ε-hcp phase appeared in the matrix.

Ni-Cr-Mo alloy is the most commonly used screw material for injection molding of F-bearing resins or plastics. However, due to its low hardness, the alloy exhibits relatively low wear resistance compared to a Co-Cr-Mo alloy, which greatly limits its application in the injection molding of some sophisticated products. Therefore, in this study [2], a novel Ni-Co-Cr-Mo alloy was developed, and the corrosion resistance of alloys with and without Co addition to an aqueous HF acid solution were compared and analyzed systematically.

This study examined the effect of partially substituting cobalt for nickel on the corrosion resistance of Ni-16Cr-15Mo in a 5.2 M HF acid solution at 100 °C. Microstructural characterization revealed that cobalt substitution did not have a detrimental effect on corrosion resistance and enhanced the formation of a thin, compact, Mo-rich passive film formed by selective dissolution of the elements.

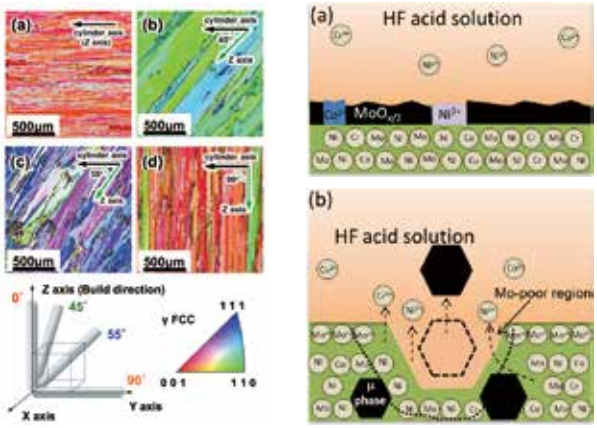

(L) Fig. 1 Inverse pole-figure maps showing the crystal orientation of a cross section of Co-Cr-Mo alloy rods fabricated using EBM whose cylinder axes deviated from the build direction by (a) 0°, (b) 45°, (c) 55° , and 90° [1].

(R) Fig. 2 (a) Proposed corrosion mechanism of Ni-(30Co)-16Cr-15Mo in HF acid solution by formation of a compact $MoO_{x/2}$ protective layer, and (b) more drastic dissolution of alloy elements surrounding μ-phase (π phase in case of Ni-16Cr-15Mo alloy) particles, resulting in final detachment of the μ phase from the alloy matrix and the severe corrosion of the alloy matrix.

Heat treatment drastically lowered the corrosion resistance as a result of the development of Mo-rich precipitates in the alloy. This also lowered the concentration of Mo in bulk matrix, in the regions near the precipitates in particular, leading to inhibition of the formation of a homogenous and compact Mo-rich passive film (Fig. 2).

References

[1] S. Sun, Y. Koizumi, S. Kurosu, Y. Li, H. Matsumoto, and A. Chiba, Acta Mater. **64**, 154 (2014).

[2] Y. Li, X. Fan, N. Tang, H. Bian, Y. Hou, Y. Koizumi, and A. Chiba, Corrosion Science **78**, 101 (2014).

Keywords: corrosion, microstructure, powder processing
Akihiko Chiba (Deformation Processing Division)
E-mail: chibalab@imr.tohoku.ac.jp
URL: http://www.chibalab.imr.tohoku.ac.jp/english/index.html

Spatially resolved Spectral Images of Microwave-induced Plasmas for Nitridation of Steel Materials

When a nitrogen microwave-induced plasma produced with an Okamoto cavity was employed as a nitridation source of steel materials, the characteristics of the plasma were investigated by analyzing spatially-resolved emission images of nitrogen excited species obtained with a two-dimensionally imaging spectrograph.

An electrodeless discharge, where a high-power microwave is coupled to a plasma gas through a surface-wave–excited non-resonant cavity developed by Okamoto [1], called Okamoto cavity, can generate nitrogen plasma at ambient pressure. Microwave-induced plasmas (MIPs) excited with an Okamoto cavity are typically used as an excitation source in atomic emission spectrometry [2,3], and especially in nitrogen/oxygen mixed gas plasmas a good analytical performance is obtained [4]. Nitrogen MIPs can also be employed as a source of nitridation [5]; the MIP elevates the substrate temperature of an iron sample due to radiative heat emanated from the plasma under an active nitrogen atmosphere, which promotes the growth of a nitrided layer on the iron substrate.

This report presents a spectroscopic observation of the Okamoto-cavity MIPs during the nitriding process and discusses the nitriding mechanisms occurring in the plasma. For this purpose, emission images for two band heads of nitrogen species, such as nitrogen molecules and nitrogen molecule ions, were measured using a two-dimensionally (2D) imaging spectrograph [6.7].

Figure 1 shows 2D emission images for a band head of nitrogen molecules at 337.13 nm (top) and of nitrogen molecule ions at 391.44 nm (bottom), at microwave forward powers of 600, 700, and 800 W [5], whose intensities are roughly described by mapping with several colors in which the intensity becomes weaker from red to blue. With increasing microwave power, the emission zone extended towards both the axial and the radial directions, and the emission intensity was enhanced at the central position of the plasma. This implies that the number density of the excited nitrogen species was elevated, which promotes the nitriding reactions occurring on the surface of an iron plate, located on a stage ca. 50 mm above the front plate of the cavity.

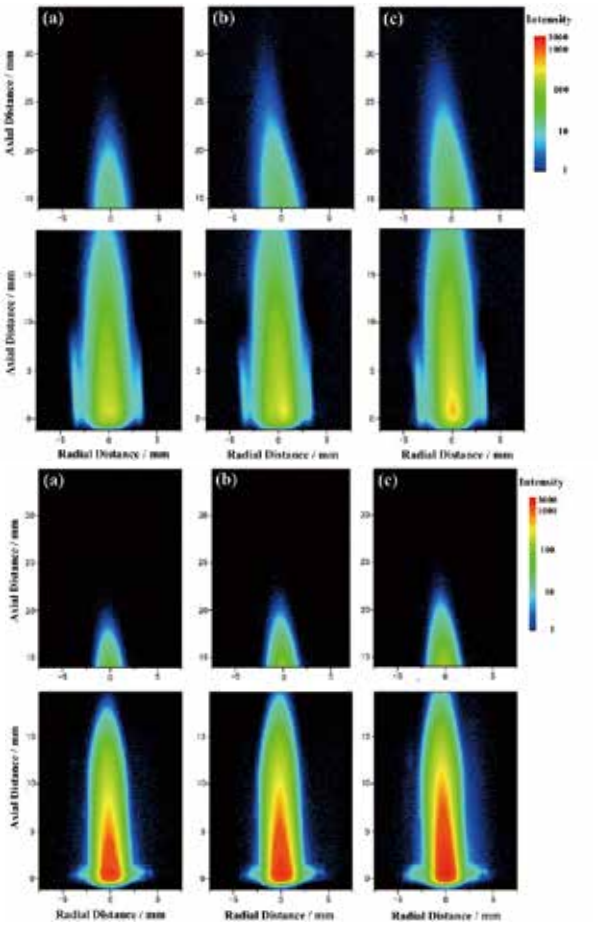

Fig.1 Two-dimensional plasma images of band heads at N_2 337.13nm (top) and N_2^+ 391.44 nm (bottom) at microwave powers of 600W (a) 700W (b) and 800W (c) After Ref. [5].

References

[1] Y. Okamoto, Anal. Sci. **7**, 283 (1991).
[2] T. Maeda and K. Wagatsuma, Microchem. J. **76**, 53 (2004).
[3] Z. Zhang and K. Wagatsuma, Spectrochim. Acta, Part B **57**, 1247 (2002).
[4] Y. Arai, S. Sato, and K. Wagatsuma, ISIJ Int. **11**, 1993 (2013).
[5] S. Sato, Y. Arai, and K. Wagatsuma, Anal. Sci. **30**, 237 (2014).
[6] C. Kitaoka and K. Wagatsuma, Anal. Sci. **23**, 1261 (2007).
[7] M. Matsuura and K. Wagatsuma, Anal. Sci. **27**, 231 (2011).

Keywords: atomic emission spectrometry, surface reaction, steel
Kazuaki Wagatsuma (Analytical Sciences Division)
E-mail: wagatuma@imr.tohoku.ac.jp
URL: http://wagatsuma.imr.tohoku.ac.jp

Towards K-computing

The Computational Materials Research Initiative (CMRI) at IMR promotes various supercomputer projects within the CMSI (Computational Materials Science Initiative) [1]. Among these projects are those designated "Priority Research Topics" and "Special Support Research Topics." Professors Kaoru Ohno (Yokohama National University) and Munekazu Ohno (Hokkaido University) are the active leading members in charge of two Special Support Research Topics projects. Recent developments in their exciting projects are described below.

Electron spectra and dynamics of ensemble functional materials, from nanoclusters to crystals

To investigate the electron spectra and dynamics of various functional materials, from nanoclusters to crystals, we have developed a computational all-electron mixed basis approach in our 'TOMBO' code, which eliminates the shortcomings of existing first-principles methods. In this approach, single-electron wave functions are expanded as a linear combination of both plane waves (PWs) and numerical atomic orbitals (AOs); see Fig. 1. Using this code, we investigated ground- and excited-state chemical reactions forming HCOOH and $Fe(OH)_2$. We also investigated the impurity level of Nb-doped TiO_2 (rutile) using the GW approximation, which can correctly reproduce the energy gap and band structure. The optical absorption spectra of different molecules were also calculated by solving the Bethe-Salpeter equation [2].

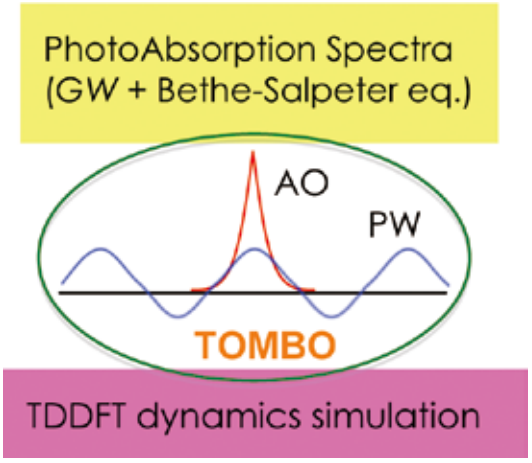

Fig. 1 The principles underlying the all-electron mixed basis code, TOMBO.

Large-scale simulation of the growth of dendrite structures during alloy solidification

Understanding the microstructure formation process during solidification, especially that of dendritic structures, is one of the most important issues in solidification science and engineering. In order to carry out a highly accurate and large scale computation of formation process of dendrite structure, we developed 1) molecular dynamics simulations for high-temperature quantities related to the solidification microstructure, such as the solid/liquid interfacial energy, 2) quantitative phase-field models, and 3) large scale phase-field simulations for dendrite structure. Figure 2 shows an example of a very large-scale phase-field simulation of the competitive growth of dendrites during unidirectional solidification. By means of this large-scale phase-field simulation, we recently clarified new aspects of the selection rules of directionally solidified dendrites [3].

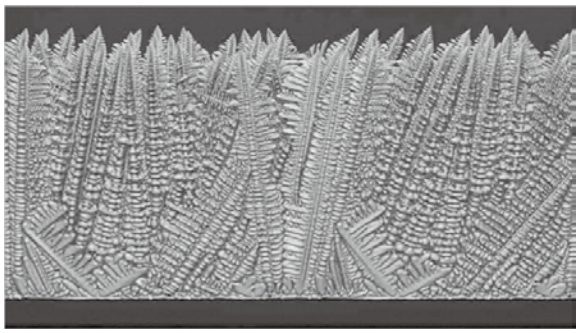

Fig. 2 The results of a very large scale phase-field simulation of dendrite structure by TSUBAME 2.0.

References

[1] T. Mohri, IMR KINKEN Research Highlights 2013 p15 (2013).
[2] M. Zhang, S. Ono, and K. Ohno, "GW calculation of electronic structure of titanium dioxide with Nb doping using TOMBO", ACCMS-VO8, Sendai/Matsushima, Nov. 7-9, 2013.
[3] T. Takaki, T. Shimokawabe, M. Ohno, A. Yamanaka, and T. Aoki, J. Crys. Growth **382**, 21 (2013).

Keywords: dendrite, casting, simulation
Tetsuo Mohri (Computational Materials Research Initiative)
E-mail: tmohri@imr.tohoku.ac.jp
URL: http://www.cmri-tohoku.jp/